Inorganic Chemistry

ARTICLE

pubs.acs.org/IC

Serine-Based Homochiral Nanoporous Frameworks for Selective CO_2 Uptake

Yan-Xi Tan, Yan-Ping He, and Jian Zhang*

State Key Laboratory of Structural Chemistry, Fujian Institute of Research on the Structure of Matter, Chinese Academy of Sciences, Fuzhou, Fujian 350002, P. R. China.

Supporting Information

ABSTRACT: Presented here are two serine-based homochiral materials that show isostructural nanoporous three-dimensional frameworks with high selectivity and storage capacity for CO_2 over N_2 and CO at ambient conditions.

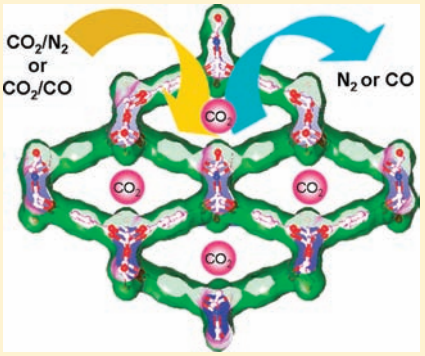

INTRODUCTION

The reduction of CO_2 in the air is now a worldwide task to avoid the greenhouse effect.[1] Selective trapping of CO_2 from air or the emissions of coal-fired power plants under ambient conditions becomes more and more important for this purpose.[2] Recently, porous metal organic framework materials (MOFs) have been considered as very promising candidate for gas storage and separation because of their high surface area and tunable structural features.[3−5] The storage of CO_2 and its selective separation from gas mixtures are two main tasks for MOF materials. Of particular interest is the efficient separation of CO_2 from N_2 at ambient temperature and pressure, because that is the key fact in the capture of carbon from flue gas. Numbers of MOF materials with selective adsorption of CO_2 over N_2 have been reported in near five years, but highly efficient materials are still rare emerging.[6,7] So far how to enhance the separation ability of the materials from structural modification approach remains great challenge. The current research efforts in this area have focused on either (1) increasing pore volume or surface area to improve CO_2 capacity or (2) modifying the physical and chemical environments in pores by introducing functional moieties with high affinity to CO_2.[8,9] It has been recognized that some specific polar groups, for example, −OH, −COOH, or $-NH_2$, can dramatically help on the selectivity of CO_2 rather than other gases (e.g., N_2, CH_4, H_2).[10] Considering the above points, what should happen if a combination of such specific polar groups in a molecular building block was realized by the porous MOF material? Unfortunately, the answer is still unknown and no related porous MOF materials are synthesized.

A special molecule containing all −OH, −COOH, and $-NH_2$ groups is serine, one of the typical amino acid. However, porous three-dimensional MOF materials based on serine have never been explored to date, although other amino acid-based porous MOFs have been reported.[11] Serine is such a functional ligand not only due to its multidentate coordinate sites, but also due to its intrinsic homochirality. MOFs constructed from commercial available enantiopure serine should take another outstanding merit on homochiral applications, such as enantioselective catalysis and separation.[11−13] Since the presence of rich polar groups, serine-based porous MOF materials may open a new approach toward the CO_2 capture and its selective separation.

Herein, we report two homochiral materials synthesized from D- or L-serine, respectively, which show isostructural nanoporous three-dimensional frameworks with high selectivity and storage capacity for carbon dioxide over nitrogen at ambient conditions.

EXPERIMENTAL SECTION

General Procedures. All the syntheses were performed in 20 mL glass vial under autogenous pressure. Reagents were purchased commercially and used without further purification. Thermal analysis was carried out on a Netzsch STA449C thermal analyzer under dinitrogen atmosphere with a heating rate of 10 °C·min^{-1}. X-ray powder diffraction experiments were performed in a Rigaku Dmax 2500 instrument with an ultra 18Kw Cu rotating anode point source. Gas adsorption measurement was performed in the ASAP (Accelerated Surface Area and Porosimetry) 2020 System.

Received: July 8, 2011
Published: October 21, 2011

Table 1. Crystal Data and Structure Refinement for 1-L and 1-D

compound reference	**1-L**	**1-D**
chemical formula	$c_{22}h_{14}n_2o_{14}zn_4$	$c_{22}h_{14}n_2o_{14}zn_4$
formula mass	791.83	791.83
crystal system	monoclinic	monoclinic
space group	*P*2(1)	*P*2(1)
a (Å)	19.293(4)	19.420(13)
b (Å)	14.332(3)	14.437(10)
c (Å)	10.3246(14)	10.337(7)
α (deg)	90.00	90.00
β (deg)	90.114(10)	89.731(13)
γ (deg)	90.00	90.00
unit cell volume	2854.8(9)	2898(3)
temperature (K)	293(2)	293(2)
Z	2	2
no. of reflections measured	23 529	24 911
no. of independent reflections	10 661	12 843
R_{int}	0.0749	0.0639
final *R*1 values ($I > 2\sigma(I)$)	0.0494	0.0713
final wR(F^2) values ($I > 2\sigma(I)$)	0.1235	0.1904
goodness of fit on F^2	0.864	0.955
Flack parameter	−0.08(5)	0.00(2)

*Synthesis of Zn_4(L-Ser)$_2$(bdc)·6DMF (**1-L**).* A mixture of $Zn(NO_3)_2 \cdot 6H_2O$ (0.595 g, 2 mmol), L-serine (L-Ser, 0.105 g, 1 mmol), terephthalic acid (H_2bdc, 0.166 g, 1 mmol), and 10 mL of *N*,*N*-dimethylformamide (DMF) was heated up and stirred to give a yellow clear solution, and then transferred and sealed in a 23 mL of Teflon-lined airtight reactor was heated at 120 °C for 2 days, and then cooled to room-temperature. Fresh DMF was used to wash the primrose yellow crystals, and the obtained crystals were stored in a desiccator.

*Synthesis of Zn_4(D-Ser)$_2$(bdc)·6DMF (**1-D**).* **1-D** was prepared by a procedure similar with that of **1-L**, except for the replacement of L-serine by D-serine.

X-ray Crystallography. The diffraction data was collected on a Saturn 70 charge-coupled device diffractometer equipped with confocal-monochromated Mo Kα radiation (λ = 0.71073 Å) at room temperature. The CrystalClear program was used for absorption correction. The structures were solved by direct methods and refined on F^2 by full-matrix, least-squares methods using the SHELXL-97 program package. All non-hydrogen atoms were refined with anisotropic displacement parameters. The total interstitial solvent molecule contents of **1** were determined by TGA. Crystal data for **1-L** and **1-D** are listed in Table 1.

RESULTS AND DISCUSSION

Compounds were synthesized, respectively, by mixing serine (D- or L-form), 1,4-benzenebicarboxlic acid (H_2bdc), and Zn-$(NO_3)_2 \cdot 6H_2O$ in a 1:1:2 molar ratio in DMF solution at 120 °C for 2 days. Single-crystal X-ray Diffraction studies reveal that they are isostructural and formulated as $[Zn_4(bdc)_2(L\text{-ser})_2)] \cdot 6DMF$ (**1-L**) and $[Zn_4(bdc)_2(D\text{-Ser})_2)] \cdot 6DMF$ (**1-D**), respectively. The phase purity of the bulk product was independently confirmed by powder X-ray diffraction (XRD).

Crystal Sructure Description. The prominent structural feature of **1-L** is that the homochiral chains built from enantiopure L-serine and Zn centers are linked together by achiral bdc ligands to form a rod-and-spacer motif with large rhombic channels. Compound **1-L** crystallized in the chiral $P2_1$ space group because of the derivation from the enantiopure L-serine. It is notable that the coordination fashion of L-serine in the structure is unprecedented, because it is a dianion owing to the deprotonation of the hydroxy group and acts as an unusual μ_4-ligand to bound four Zn^{2+} ions (Figure 1a). The interesting point is that the $-NH_2$ group of L-serine bridges two Zn centers with the Zn···Zn distance being 3.52 Å. Each five-coordinate Zn center (ZnO_4N) has distorted trigonal bipyramid geometry, and they are connected by the L-serine ligands into a homochiral chain along the *c* axis (Figure 1a). Meanwhile, the achiral bdc

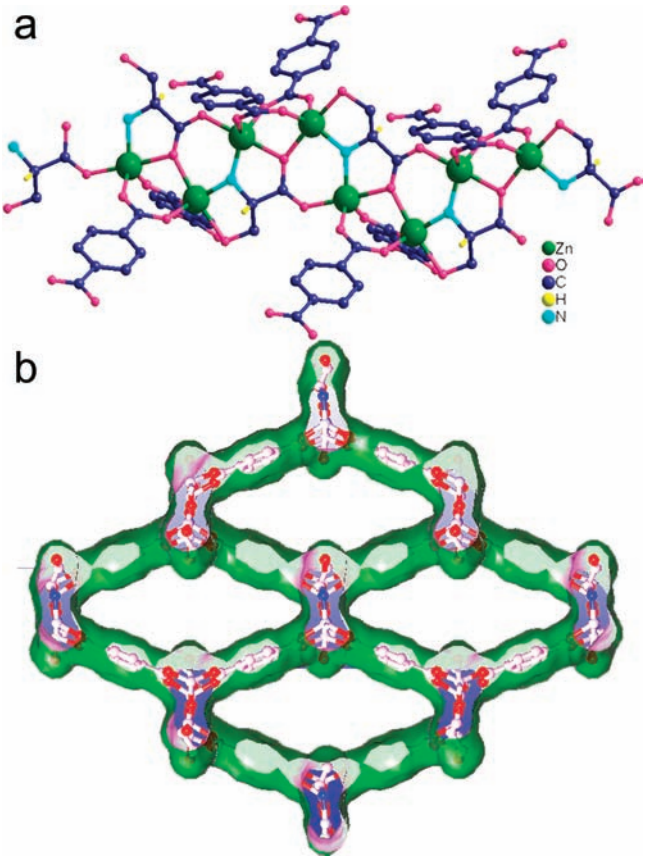

Figure 1. (a) Coordination environment of Zn atom in **1-L**. (b) The 3D porous framework viewed along the *c* axis.

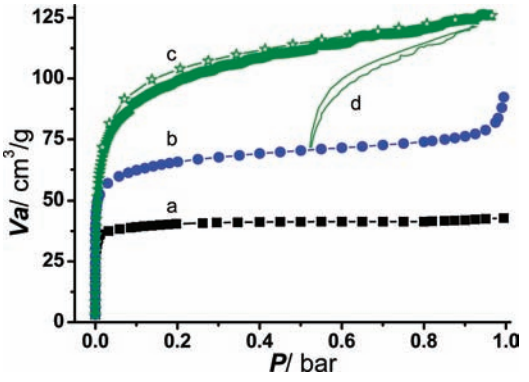

Figure 2. N_2 and CO_2 adsorption isotherms: (a) N_2 at 77 K for **1-L-ht**, (b) N_2 at 77 K for **1′-L-ht**, (c) CO_2 at 195 K for **1-L-ht**, and (d) the hysteresis loop of CO_2 at 195 K for **1-L-ht**.

dx.doi.org/10.1021/ic201442u |*Inorg. Chem.* 2011, 50, 11527–11531

Table 2. Adsorption Data and Isosteric Heat Data for 1-L-ht and Í-L-ht

compound	BET[a]	CO_2@273 K[b]	CO_2@298 K[b]	$Q_{st}(CO_2)$[c]	$S(CO_2/N_2)$@273 K[d]	H_2@77 K[b]	H_2@87 K[b]	$Q_{st}(H_2)$[c]
1-L-ht	136.9	55.5	37.1	32.1	185	105.8	79.8	8.2
1′-L-ht	224.7	43.7	30.3	28.6	17.5	66.7	50.7	7.5

[a] Surface area, m^2/g. [b] Adsorptive capability, mL/g. [c] Isosteric heat of adsorption at 1 bar, kJ/mol. [d] Selectivity of CO_2 over N_2, v/v.

ligands, whose oxygen atoms occupy the equatorial positions of the homochiral chains, further bridge these parallel homochiral chains to form a neutral 3D framework with large channels along the *c* axis (Figure 1b). The effective size of this rhombic window for each channel is about 20 × 10 $Å^2$ by measuring the diagonal centers. A large void is generated within the channels with the V_{void} without guest DMF molecules of 63.3% as calculated by PLATON.[14] The channels are occupied by the structural disordered DMF molecules. There are six DMF guest molecules per formula unit of the host, as evidenced by thermal gravimetric (TG) analysis data. Compound **1-D** prepared from D-serine is the enantiomorphism of **1-L** and has similar homochiral structure (space group: $P2_1$) to **1-L**. The framework structure of **1-L** is also similar to the reported compound [Zn_2(bdc)(L-lactate)-(DMF)]·DMF where the L-lactate ligand was used and each Zn center is coordinated by one solvent DMF molecule.[12] In **1-L**, the −OH group of L-serine acted as a tailor and replaced the coordination site of DMF in that reported compound. Thus it becomes much easier for **1-L** to remove the solvent DMF molecules from the pores.

Thermal Stability. Thermal gravimetric analyses (TGA) and X-ray powder diffraction pattern (XRPD) measurements were carried out to examine the thermal stability of this nanoporous framework. The TGA curve of **1-L** shows that the trapped solvent DMF molecules can be drastically removed at 250 °C with a weight loss of 35.4% (calculated 35.6%) (Supporting Information Figure S2a). The hollow phase (**1-L-ht**) of **1-L** was obtained after heated at 180 °C for 7 h under high vacuum (10^{-8} mbar), the powder X-ray diffraction pattern of **1-L-ht** have appeared obvious change (Supporting Information Figure S3c). It may be due to the laxity of **1-L** after the removal of DMF guests. To attain a more complete evacuation and protect the structural integrality, DMF was exchanged with methanol by soaking crystals of **1-L** in methanol for one week. As indicated by TGA and infrared spectroscopy, the methanol activated material **1′-L** is DMF free (Supporting Information Figures S2b and S4). Its TGA curve showed that methanol was released below 100 °C. Its hollow phase (**1′-L-ht**) was obtained after heated at 80 °C for 7 h under high vacuum.

Gas Sorption Properties. The permanent porosity of **1-L-ht** was established by reversible gas sorption experiments using N_2 and CO_2 at 77 and 195 K, respectively, which all show a typical type I behavior characterized by a plateau reached at low relative pressure indicating the presence of permanent micropores in **1-L-ht** (Figure 2 and Table 2). The lower uptake of N_2 (42 cm^3/g) and higher uptake of CO_2 (127 cm^3/g) may be induced by the strong polar environment in the pores. N_2 adsorption data gives a BET surface area of 136.9 m^2/g and a Langmuir surface area of 180.4 m^2/g. A single data point at relative pressure 0.295 gives a maxima pore volume of 0.063 cm^3/g by the Horvath−Kawazoe equation. Comparatively, the maximum N_2 uptakes at 1 bar for **1′-L-ht** are 92.3 cm^3/g (STP), giving a BET surface area of 224.7 m^2/g and a Langmuir surface area of 298.5 m^2/g, which are all much larger than that for **1-L-ht**. A single data point at relative pressure 0.01 gives a maxima pore volume of 0.081 cm^3/g by the Horvath−Kawazoe equation. The results demonstrate the importance of activation for porous materials.

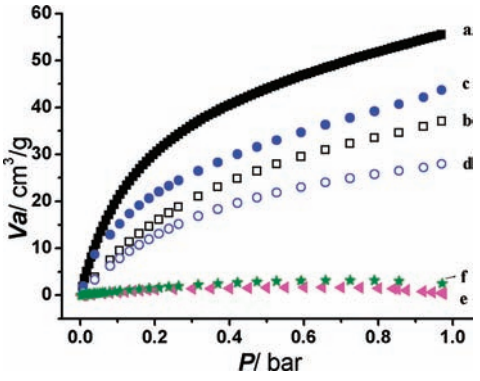

Figure 3. N_2 and CO_2 adsorption isotherms: (a) CO_2 at 273 K for **1-L-ht**, (b) CO_2 at 298 K for **1-L-ht**, (c) CO_2 at 273 K for **1′-L-ht**, (d) CO_2 at 298 K for **1′-L-ht**, (e) N_2 at 273 K for **1-L-ht** and (f) N_2 at 273 K for **1′-L-ht**.

It is worth noting that there is a small hysteresis loop for the CO_2 sorption of **1-L-ht**, suggesting relatively strong adsorbent−adsorbate interactions between the framework and CO_2.[15] This phenomenon encourages us to further explore its potential properties on CO_2/N_2 gas separation under ambient conditions. The adsorption isotherms of CO_2 and N_2 for **1-L-ht** and **1′-L-ht** at 273 K were measured, respectively (Figure 3, Table 2). The uptake value of CO_2 for **1-L-ht** was 55.5 cm^3/g (2.49 mmol/g and 109.2 mg/g), which is comparable to the well-known MOF-5 and larger than many other reported compounds.[7a] However, the CO_2 uptake of 43.7 cm^3/g for **1′-L-ht** is much less than that of **1-L-ht**. In particular, CO_2 uptake (42.1 mg/g at 273 K) of **1-L-ht** at 0.1 bar, a typical partial pressure of CO_2 in flue gases from power plants and steel mills, is comparable or even superior to that of many MOFs.[2] To better understand these observations, the adsorptive capability of **1-L-ht** and **1′-L-ht** were measured under 298 K, giving an uptake of 37.1 cm^3/g for **1-L-ht** and 21.4 cm^3/g for **1′-L-ht** (Figure 3b and 3d). The enthalpy of CO_2 adsorption for **1-L-ht** was estimated from the sorption isotherms at 273 and 298 K using the virial equation to understand the strong affinity of **1-L-ht** toward CO_2 (Supporting Information Figures S5 and S6). At zero coverage, the enthalpy of CO_2 adsorption is 32.1 kJ/mol for **1-L-ht** and 28.6 kJ/mol for **1′-L-ht**, which is comparable to those of MOFs with organic ammonium ions in the pores for strong CO_2 binding.[9b] In contrast, N_2 was hardly adsorbed at all under the conditions of 273 K (just 0.3 cm^3/g for **1-L-ht** and 2.5 cm^3/g for **1′-L-ht**). The maximal uptakes of the CO_2 and N_2 at 273 K and 1 bar for **1-L-ht** were used to estimate the adsorption selectivity for CO_2 over N_2.[16] From these data, the calculated CO_2/N_2 selectivity is 185:1 for **1-L-ht** and 17.5:1 for **1′-L-ht** at 273 K. MOFs with such high CO_2/N_2 adsorption selectivity at ambient conditions were rarely reported.[17]

dx.doi.org/10.1021/ic201442u |*Inorg. Chem.* 2011, 50, 11527–11531

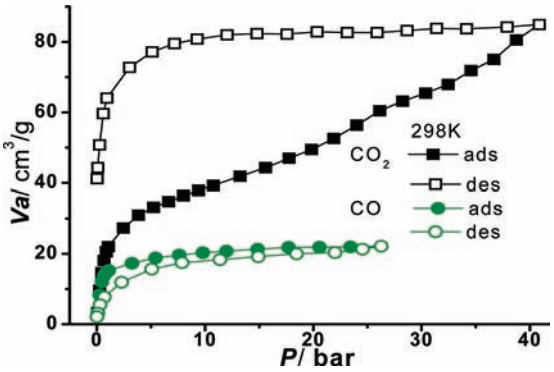

Figure 4. High-pressure adsorption isotherms of CO_2 and CO at 298 K for **1-L-ht**.

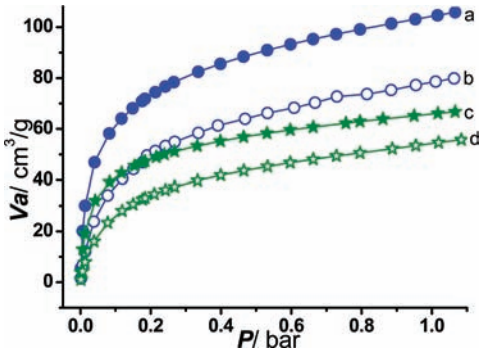

Figure 5. H_2 adsorption isotherms: (a) H_2 at 77 K for **1-L-ht**, (b) H_2 at 87 K for **1-L-ht**, (c) H_2 at 77 K for **1′-L-ht**, (d) H_2 at 87 K for **1′-L-ht**.

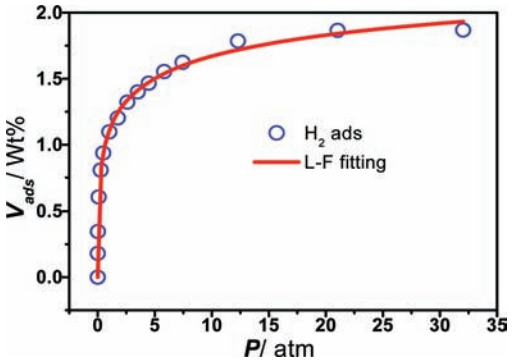

Figure 6. H_2 adsorption isotherm for **1-L-ht** recorded at 77 K, and the red solid line is the fitting of the H_2 adsorption isotherm of **1-L-ht** using Langmuir−Freundlich equation.

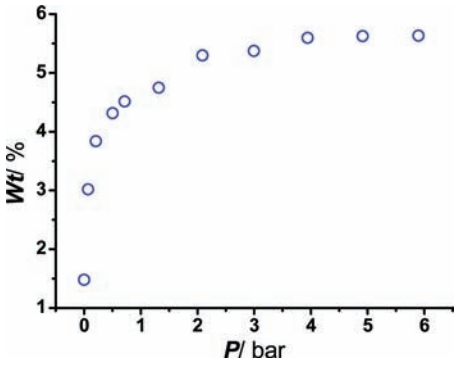

Figure 7. CH_4 adsorption isotherm for **1-L-ht** recorded at 273 K.

In view of the structural feature of **1-L**, such gas-adsorption selectivity might be associated with the presence the π-electrons of the ligands and the polar $-NH_2$ groups, giving rise to an electric field to induce a dipole in CO_2 and an interaction between CO_2 and $-NH_2$.[10] The presence of the μ_2-NH_2 groups and C═O groups of neighboring ligands provides chances on the inteaction betwwen of CO_2 and $-NH_2$.[9c] These cooperative effects yield an enhanced lone pair polarization of the CO_2 electron density, highlighting the impact of the specific pore geometry in the structure of **1-L**.

The high-press sorption experiments of CO_2 and CO were also measured at 298 K for **1-L-ht**, which show distinct sorption behavior. The CO_2 uptake by **1-L-ht** at 40 bar can reach 84 cm^3/g (3.75 mmol/g) and are not fully saturated, while the saturated uptake of CO is limited to 22 cm^3/g (0.98 mmol/g) at 26 bar (Figure 4). Interestingly, there is significant hysteresis for CO_2 sorption whereas it is opposite for CO sorption. The significant hysteresis for **1-L-ht** may be attributed to the dynamic feature of the host framework. The selective adsorption of CO_2 over CO may be attributed to the sorbate−sorbent affinity between the CO_2 molecules and the polar framework.

Low-pressure H_2 adsorption isotherms collected for samples of **1-L-ht** and **1′-L-ht** indicated that the framework had a strong affinity for binding H_2 (Table 2 and Figure 5). At 77 K and 1.06 bar (800 Torr), a fully reversible uptake of 105.8 mL/g H_2 for **1-L-ht** but 66.7 cm^3/g H_2 for **1′-L-ht** are apparent. As a further test, a second H_2 adsorption isotherm was measured at 87 K, and the two data sets were used to determine the isosteric heat of H_2 adsorption. The enthalpy of H_2 adsorption for **1-L-ht** and **1′-L-ht** and was estimated from the sorption isotherms at 77 and 87 K using the virial equation to understand the affinity of **1-L-ht** and **1′-L-ht** toward H_2 (Supporting Information Figure S8−10). The isosteric heat of H_2 adsorption for **1-L-ht** and **1′-L-ht** reach the values of 8.2 and 7.5 kJ/mol.

What is more, the gravimetric H_2 and CH_4 sorption isotherms of **1-L-ht** were also measured at 77 and 273 K, respectively. The H_2 sorption on **1-L-ht** showed type-I sorption behavior indicatives of the filling of the micropores only. The capacity of **1-L-ht** to adsorb H_2 increases to a saturation of 1.87 wt % at 32 bar (Figure 6), and the adsorption amounts of CH_4 is 5.64 wt % at 6 bar (Figure 7). In addition, the density of the maximum adsorbed H_2 (2.77 wt %, obtained by fitting of the Langmuir−Freundlich (L−F) equation to the adsorption isotherm.) is much higher than the experimental value (1.87 wt %).

CONCLUSION

In summary, two serine-based homochiral nanoporous framework materials were successfully synthesized and **1-L** exhibited high selectivity and storage capacity for CO_2 over N_2 and CO at ambient conditions. The results indicated the special coordination mode of serine ligand and its functionality on CO_2 uptake. This work also revealed that a flexible framework material with suitable pore size and polar functional groups may be a good candidate for the application in CO_2/N_2 separation.

ASSOCIATED CONTENT

Supporting Information. Additional figures, TGA, powder X-ray diffraction patterns, IR spectra, sorption isotherms, and

CIF files. This material is available free of charge via the Internet at http://pubs.acs.org.

AUTHOR INFORMATION

Corresponding Author
*E-mail: zhj@fjirsm.ac.cn.

ACKNOWLEDGMENT

We thank the support of this work by National Basic Research Program of China (973 Programs 2011CB932504 and 2012-CB821705), NSFC (21073191), NSF of Fujian Province (2011J06005) and the Innovation Program of CAS (KJCX2-YW-H21).

REFERENCES

(1) Stern, N. *Stern Review on the Economics of Climate Change*; Cambridge University Press: Cambridge, 2006.
(2) D'Alessandro, D. M.; Smit, B.; Long, J. R. *Angew. Chem., Int. Ed.* **2010**, *49*, 6058.
(3) (a) Férey, G. *Chem. Soc. Rev.* **2008**, *37*, 191. (b) Cheon, Y. E.; Park, J.; Suh, P. *Chem. Commun* **2009**, 5436. (c) Zhang, J.; Wu, T.; Zhou, C.; Chen, S.; Feng, P.; Bu, X. *Angew. Chem., Int. Ed.* **2009**, *48*, 2542.
(4) (a) Li, J.-R.; Kuppler, R. J.; Zhou, H.-C. *Chem. Soc.Rev.* **2009**, *38*, 1477. (b) Park, H. J.; Suh, M. P. *Chem. Commun* **2010**, *46*, 610. (c) Zeng, M.-H.; Wang, Q.-X.; Tan, Y.-X.; Hu, S.; Zhao, H.-X.; Long, L.-S. *J. Am. Chem. Soc.* **2010**, *132*, 2561.
(5) (a) Ma, L.; Lin, W. *Angew. Chem., Int. Ed.* **2009**, *48*, 3637. (b) Ma, L.; Mihalcik, D. J.; Lin, W. *J. Am. Chem. Soc.* **2009**, *131*, 4610. (c) Ma, S.; Yuan, D.; Chang, J.-S.; Zhou, H.-C. *Inorg. Chem.* **2009**, *48*, 5398. (d) Chen, B.; Ma, S.; Zapata, F.; Fronczek, F. R.; Lobkovsky, E. B.; Zhou, H.-C. *Inorg. Chem.* **2007**, *46*, 1233. (e) Chen, B.; Ma, S.; Hurtado, E. J.; Lobkovsky, E. B.; Liang, C.; Zhu, H.; Dai, S. *Inorg. Chem.* **2007**, *46*, 8705.
(6) (a) Banerjee, R.; Furukawa, H.; Britt, D.; Knobler, C.; O'Keeffe, M.; Yaghi, O. M. *J. Am. Chem. Soc.* **2009**, *131*, 3875. (b) Guo, Z.; Wu, H.; Gadipelli, S.; Liao, T.; Zhou, Y.; Xiang, S.; Chen, Z.; Yang, Y.; Zhou, W.; O'Keeffe, M.; Chen, B. *Angew. Chem., Int. Ed.* **2011**, *50*, 3178. (c) Chen, B.; Xiang, S.; Qian, G. *Acc. Chem. Res.* **2010**, *43*, 1115.
(7) (a) Demessence, A.; D'Alessandro, D. M.; Foo, M. L.; Long, J. R. *J. Am. Chem. Soc.* **2009**, *131*, 8784. (b) Bae, Y. S.; Farha, O. K.; Hupp, J. T.; Snurr, R. Q. *J. Mater. Chem.* **2009**, *19*, 2131.
(8) Caskey, S. R.; Wong-Foy, A. G.; Matzger, A. *J. Am. Chem. Soc.* **2008**, *130*, 10870.
(9) (a) An, J.; Fiorella, R. P.; Geib, S. J.; Rosi, N. L. *J. Am. Chem. Soc.* **2009**, *131*, 8401. (b) An, J.; Rosi, N. L. *J. Am. Chem. Soc.* **2010**, *132*, 5578. (c) Vaidhyanathan, R.; Iremonger, S. S.; Shimizu, G. K. H.; Boyd, P. G.; Alavi, S.; Woo, T. K. *Science* **2010**, *330*, 650.
(10) Torrisi, A.; Bell, R. G.; Mellot-Draznieks, C. *Cryst. Growth Des.* **2010**, *10*, 2839.
(11) (a) Vaidhyanathan, R.; Bradshaw, D.; Rebilly, J.-N.; Barrio, J. P.; Gould, J. A.; Berry, N. G.; Rosseinsky, M. J. *Angew. Chem., Int. Ed.* **2006**, *45*, 6495. (b) Chen, L.; Bu, X. *Chem. Mater.* **2006**, *18*, 1857–1860.
(12) Dybtsev, D. N.; Nuzhdin, A. L.; Chun, H.; Bryliakov, K. P.; Talsi, E. P.; Fedin, V. P.; Kim, K. *Angew. Chem., Int. Ed.* **2006**, *45*, 916.
(13) Ma, L.; Abney, C.; Lin, W. *Chem Soc. Rev.* **2009**, *38*, 1248.
(14) Spek, A. L. *J. Appl. Crystallogr.* **2003**, *36*, 7.
(15) Lee, J. Y.; Pan, L.; Huang, X.; Emge, T. J.; Li, J. *Adv. Funct. Mater.* **2011**, *21*, 993.
(16) Jin, Y.; Voss, B. A.; Noble, R. D.; Zhang, W. *Angew. Chem., Int. Ed.* **2010**, *49*, 6348.
(17) Sumida, K.; Horike, S.; Kaye, S. S.; Herm, Z. R.; Queen, W. L.; Brown, C. M.; Grandjean, F.; Long, G. J.; Dailly, A.; Long, J. R. *Chem. Sci.* **2010**, *1*, 184.